Received: 14 December 2023 | Accepted: 6 February 2024

DOI: 10.1111/1759-7714.15257

ORIGINAL ARTICLE

WILEY

CircCPA4 induces ASCT2 expression to promote tumor property of non-small cell lung cancer cells in a miR-145-5p-dependent manner

Zhenhua Zhang[1] | Weiliang Liu[1] | Tao Huang[1] | Junyan Li[1] | Hui Hu[1] | Xinyu Xu[1] | Zhigang Fan[2]

[1]Department of Cardiothoracic Surgery, Hanzhong, China

[2]Department of Oncology, Hanzhong, China

Correspondence
Zhigang Fan, Department of Oncology, 3201 Hospital, No. 783 Tianhan revenue, Hantai district 723000, Hanzhong, Shaanxi, China.
Email: nzymb5@163.com

Funding information
Key R&D Plan of Shaanxi Province, Grant/Award Number: 2021SF-044

Abstract

Background: Non-small cell lung cancer (NSCLC) is a type of lung cancer that occurs in the cells of the respiratory tract, and its development is influenced by the regulation of circular RNAs (circRNAs). However, the role of circRNA carboxypeptidase A4 (circCPA4) in the progression of NSCLC and the underlying mechanism remain relatively clear.

Methods: The study utilized both real-time quantitative polymerase chain reaction (RT-qPCR) and western blot techniques to evaluate the levels of circCPA4, microRNA-145-5p (miR-145-5p), alanine, serine, or cysteine-preferring transporter 2 (ASCT2). To assess cell proliferation, cell counting kit-8 (CCK8) and 5-ethynyl-2′-deoxyuridine (EdU) assays were performed. Apoptosis was determined using flow cytometry, while cell migration and invasive capacity were evaluated through transwell and wound-healing assays. Intracellular levels of glutamine, glutamate, and α-KG were measured using specific kits. The relationship between miR-145-5p and circCPA4 or ASCT2 was confirmed using dual-luciferase reporter assay and RNA immunoprecipitation assay.

Results: CircCPA4 and ASCT2 RNA levels were elevated, while miR-145-5p was downregulated in both NSCLC tissues and cells. Depletion of circCPA4 significantly inhibited NSCLC cell proliferation, migration, invasion, and intracellular levels of glutamine, glutamate, and α-KG, and promoted apoptosis. Moreover, circCPA4 knockdown delayed tumor growth in vivo. Furthermore, circCPA4 was found to bind to miR-145-5p, thereby regulating the progression of NSCLC in vitro. ASCT2 was also identified as a downstream target of miR-145-5p, and its upregulation rescued the effects of miR-145-5p overexpression on NSCLC cell processes.

Conclusion: CircCPA4 knockdown inhibited tumor property of NSCLC cells by modulating the miR-145-5p/ASCT2 axis.

KEYWORDS
ASCT2, circCPA4, miR-145-5p, non-small cell lung cancer

INTRODUCTION

Lung cancer has a high incidence rate globally, with statistics indicating that more than 2.2 million patients were diagnosed with lung cancer in 2020, accounting for more than 11% of all cancers. In addition, lung cancer accounted for 18% of all cancer deaths in 2020, particularly among those with advanced stages of this disease.[1] Non-small cell lung cancer (NSCLC) accounts for more than 85% of all lung cancers.[2] The five-year survival rate for patients with early-stage NSCLC is around 75%, while patients with advanced NSCLC have shorter overall survival rates despite

great advances in medical technology.[3] Tobacco is a major cause of lung cancer.[4] The main treatment for NSCLC is commonly a combination of surgery and radiotherapy, but the frequent occurrence of multidrug resistance has led to a poor prognosis for NSCLC patients. Therefore, the search for effective molecular targets for NSCLC therapy should be actively conducted in the future to reduce the mortality rate.

CircRNAs are endogenous transcripts with loop-like structures and their expression varies greatly among different species.[5] CircRNAs have various functions, including acting as miRNA sponges or competing endogenous RNAs (ceRNAs) to regulate gene expression. In the circRNA-miRNA-mRNA interaction network, circRNAs act as natural miRNA sponges by binding to miRNA molecules, sequestering them and preventing their interaction with target mRNAs.[6] This interaction can modulate the availability of miRNAs and subsequently impact the expression of target genes. The dysregulation of this circRNA-miRNA-mRNA crosstalk has been implicated in various aspects of cancers such as breast cancer[7] and lung cancer.[8] Currently, circRNAs have emerged as ideal markers for disease diagnosis and prognosis owing to their high stability.[9] Dysregulation of circRNAs has been observed in multiple cancers and linked to disease progression. For example, circ-SMARCA5 was downregulated in breast cancer tissues, and its upregulation enhanced chemotherapy sensitivity.[10] In bladder cancer (BCa), circ-ZKSCAN1 level was negatively correlated with patient survival, pathological stage and prognosis, and circ-ZKSCAN1 overexpression restrained BCa cell progression through the miR-1178-3p/p21 axis.[11] In pancreatic cancer, circ-IARS was upregulated in metastatic tissues and contributed to cancer cell metastasis and shorter survival.[12] CircRNA carboxypeptidase A4 (circCPA4, circRNA ID hsa_circ_0082374) has been identified as a promoter of lung cancer progression, but its specific mechanism of action remains unclear.[13] Our study aimed to explore the function and mechanism of circCPA4 in NSCLC.

MicroRNAs (miRNAs) exert various regulatory roles by inhibiting downstream genes at the post-transcriptional level.[14] There are currently ~2000 identified miRNAs in humans, and they are abundantly expressed in various tissues. Mounting evidence has unveiled that miRNAs participate in tumor carcinogenesis. For example, miR-155 was upregulated and acted as an oncogene in various cancers.[15,16] In bladder cancer, miR-31-5p was prominently downregulated and suppressed tumor resistance.[17] Numerous miRNAs were dysregulated in NSCLC. miR-96-5p was substantially upregulated and mediated NSCLC development by targeting RASSF8.[18] Another miRNA, miR-145-5p, was downregulated in NSCLC, as predicted through the TCGA database.[19] Our study further investigated the mechanisms of miR-145-5p in NSCLC.

ASCT2, known as SLC1A5, is a key gene involved in the transport of neutral amino acids such as glutamine and leucine. It serves as a glutamine transporter in human cells.[20] Tumor cells are characterized by enhanced metabolism, especially glycolysis and glutamine metabolism.[21] ASCT2 plays an essential regulatory role in glutamine metabolism and is significantly upregulated in various cancers.[22] Animal experiments have shown that ASCT2 silencing significantly curbed tumor growth rate, indicating its oncogenic functions in tumor-associated pathological processes.[23] In our study, we aimed to explore the function and novel mechanism of ASCT2 in NSCLC.

METHODS

Patients and samples

Tumor tissues ($n = 80$) and paracancerous tissues ($n = 80$) were harvested from 80 NSCLC patients who were treated at the 3201 Hospital. These samples were frozen in liquid nitrogen. Signed consent forms were obtained from all patients. All cellular and animal experiments in this project were approved by the Ethics Committee of the 3201 Hospital (IRB no.2022SX112, 2022.6.12).

Cell culture and transfection

Normal human bronchial epithelioid cells (16HBE cells) and NSCLC cells (A549 cells and H1299 cells) were obtained from the China Center for Type Culture Collection (Wuhan, China). H1299 cells are positive for keratin and vimentin but are negative for neurofilament triplet protein. The cells harbor a homozygous partial deletion in the p53 protein, resulting in the lack of p53 protein expression. Additionally, H1299 cells are capable of producing neuromedin B. Cells were cultured in 89% Dulbecco's modified Eagle medium (DMEM: Invitrogen) at 37°C. The siRNAs of circCPA4 (si-circCPA4) and ASCT2 (si-ASCT2), short hairpin RNA targeting circCPA4 (sh-circCPA4) and negative controls, miR-145-5p mimic, miR-145-5p inhibitor and negative controls (mimic NC and inhibitor NC), and pcDNA-ASCT2 and control (pcDNA) were purchased from GenePharma. Cell transfection was executed following the instructions of lipofectamine 2000 (Invitrogen).

RNA extraction and real-time quantitative polymerase chain reaction (RT-qPCR)

TRIzol (Invitrogen) was applied to execute RNA extraction, and the synthesis of cDNAs was conducted using miScript RT reagents (TaKaRa). Later, 1 μg of cDNA and SYBR (TaKaRa) were used to carry out RT-qPCR, and the data were processed using the $2^{-\Delta\Delta Ct}$ method. Specific primer sequences are presented in Table 1.

Identification of circRNA structure

Five micrograms of RNA from the test group were incubated with 3 U/μg of RNase R (Geneseed) for 30 min at

TABLE 1 Primers sequences used for PCR.

Name		Primers for PCR (5′-3′)
hsa_circ_0082374	Forward	CCTGCCTAGGATTTGTACAGCA
	Reverse	ATTTGGGTCAGCACCAATGC
SLC1A5 (ASCT2)	Forward	GAGACTCCAAGGGGCTCGC
	Reverse	CACAAGCAGGTTGGCTCGAAG
miR-145-5p	Forward	GCCGAGGTCCAGTTTTCCCAGGA
	Reverse	CTCAACTGGTGTCGTGGAG
β-actin	Forward	CTTCGCGGGCGACGAT
	Reverse	CCACATAGGAATCCTTCTGACC
U6	Forward	CTCGCTTCGGCAGCACA
	Reverse	AACGCTTCACGAATTTGCGT
CPA4	Forward	CCTGCAGGCCCTTTTAGACA
	Reverse	TCAGGAAAGTCTGCGGCAAT

Abbreviation: PCR, polymerase chain reaction.

37°C. Five micrograms of RNA from the control group was left untreated with RNase R. RT-qPCR was subsequently executed to analyze circCPA4 and linear CPA4 levels. NSCLC cells were incubated with 2 μg/mL of actinomycin D. After coincubation, RNA was extracted from the cells, and circCPA4 level was evaluated using RT-qPCR.

Cell counting kit-8 (CCK8) assay

Cells were grown in 96-well plates for 24, 48 or 72 h, and 10 μL of CCK8 reaction solution (Beyotime) was coincubated with the cells for 1 h. The optical density value at 450 nm was examined using a microplate reader (Bio-Rad Laboratories Inc.).

5′-ethynyl-2′-deoxyuridine assay

After 24 h of cell culture in 96-well plates, 1 × 5′-ethynyl-2′-deoxyuridine (EdU) working solution (Beyotime) was added to the cells to label them. The cells were fixed with 4% paraformaldehyde (Solarbio) and eluted with phosphate buffered saline (PBS). Click reaction solution (Beyotime) was added and incubated for 30 min in darkness. 4′,6-diamidino-2-phenylindole (DAPI: Beyotime) staining solution was added to stain the nuclei. The cells were observed under a fluorescence microscope for analysis (scale bar = 50 μm).

Apoptosis analysis

After transfection, the cells were trypsinized, and ~50 000 cells were centrifuged. The supernatant was removed, and the cells were incubated with 195 μL of binding buffer (Beyotime). Next, 5 μL of annexin V-FITC (Beyotime) and PI (Beyotime) were added and incubated for 15 min. The apoptotic cells were analyzed using a flow cytometer.

Transwell assay

For migration assay, NSCLC cells were inoculated in the upper chambers of the transwell chambers (Corning) supplemented with serum-free medium. After 24 h, the cells that migrated into the lower chambers were fixed with 4% paraformaldehyde and stained with 0.1% crystal violet (Solarbio). Subsequently, the cells were observed and evaluated using a microscope. For cell invasion assay, Matrigel matrix (Corning) was used, while the incubation time was extended to 48 h.

Wound-healing assay

NSCLC cells were cultured in six-well plates until 90% confluence. Then, pipette tips were used to make scratches. The cells were eluted with PBS and photographed using a microscope. After 48 h, the scratch width was recorded and then photographed under a microscope according to the published method.[24]

Western blot

Total protein extraction was conducted using RIPA lysis solution (Beyotime) and quantitative analysis of protein concentrations was carried out in accordance with the instruction of the BCA protein assay kit (Beyotime). After that, protein lysates were separated by 10% SDS-PAGE and then transferred to polyvinylidene difluoride (PVDF) membranes (Beyotime). The PVDF membranes were incubated with primary antibodies against E-cadherin (ab40772, 1:10000, Abcam), vimentin (ab92547, 1:1000, Abcam), β-actin (ab8226, 1:1000, Abcam) and ASCT2 (ab237704, 1:1000, Abcam) at 4°C. The immunoblot was then analyzed using enhanced chemiluminescence reagents (Millipore Corporation).

Dual-luciferase activity assay

The online database StarBase (http://starbase.sysu.edu.cn/) was used to predict the target miRNAs of circCPA4 and the target genes of miR-145-5p. Sequences of ASCT2 3′UTR and circCPA4 with miR-145-5p complementary binding sites and mutant ASCT2 3′UTR and circCPA4 without miR-145-5p-binding sites were synthesized and cloned into the psi-check2 vectors (Invitrogen) to obtain recombinant circCPA4 wt, circCPA4 mut, ASCT2 3′UTR wt and ASCT2 3′UTR mut. These plasmids were cotransfected with miR-145-5p mimic or mimic NC into 293T cells for 24 h, and luciferase activity was measured by the dual luciferase assay kit (Solarbio).

RNA immunoprecipitation assay

After trypsin digestion, the cells were collected and the supernatant was removed by centrifugation based on

the guidebook of the EZ-Magna RNA immunoprecipitation (RIP) kit (Millipore). The cells were then suspended in 500 μL of RIP and the supernatant of the cell lysate was incubated with magnetic beads coupled with Ago2 antibody (ab186733, Abcam) or IgG antibody (ab172730, Abcam) overnight at 4°C. Subsequently, the magnetic beads were washed with PBS, and the complex was purified. The contents of circCPA4 and miR-145-5p were analyzed by RT-qPCR.

Glutamine, glutamate and α-KG content determination

NSCLC cells were grown in DMEM medium with 2 mM glutamine. After 24 h, the supernatant was collected by centrifugation at 4°C. Glutamine Assay kit (ab197011, Abcam) was applied to analyze intracellular glutamine level. In brief, the collected supernatant and Gln Standard solution were added to the desired wells in 96-well plates. The hydrolysis mixture was added to each well and coincubated with the supernatant and Gln Standard for 30 min. Then, the reaction mixture was added to each well and incubated in the dark. Finally, a microplate reader was applied to determine the absorbance at 450 nm. Gln Standard solution was used to prepare the standard curve.

The glutamate assay kit (ab83389, Abcam) was used to assess the intracellular glutamate content. In brief, NSCLC cells were collected and washed using cold PBS. The cells were resuspended in 100 μL assay buffer and incubated for 20 min on ice. The supernatant was collected by centrifuging at 4°C for 5 min and then transferred to a clean tube. Standard dilutions, samples and glutamate assay buffer were added to each well, respectively. Then,100 μL of reaction mix was added to standard and sample wells, and 100 μL of background reaction mix was added to background sample wells. The incubation was performed at 37°C for 30 min, and the absorbance at 450 nm was then analyzed using a microplate reader.

Intracellular α-KG level was analyzed with the application of the alpha ketoglutarate assay kit (ab83431, Abcam). Briefly, NSCLC cells were harvested and resuspended in 500 μL of alpha KG assay buffer. Cell supernatant was collected by centrifugation at 10 000 × g for 5 min. Cold PCA was added to each well and incubated for 5 min. After centrifugation at 10 000 × g for 2 min, the supernatant was transferred to fresh tubes. Then, 2M KOH was added to wells, and samples were centrifuged at 10 000 × g for 15 min. Reaction mix and background reaction mix were added to wells according to the guidebook, and the absorbance at 570 nm was finally measured using a microplate reader.

Xenograft model

A xenograft mouse model assay was approved by the Animal Care Committee of 3201 Hospital. A total of 10 mice were purchased from Vital River Laboratory Animal Technology (35 days; Beijing, China) and randomly distributed into two groups (sh-circCPA4 group and sh-NC group). Then, the posterior part of the mouse armpit was injected with A549 cells stably transfected with sh-circCPA4 or sh-NC. The volume was calculated weekly following the formula: volume = width^2 × length/2. After 4 weeks, the mice were euthanized with pentobarbital and the tumor tissues were collected, weighed, photographed, and stored in liquid nitrogen.

Immunohistochemistry assay

Paraffin sections were incubated with Xylene (Solarbio) for 25 min for dewaxing. They were then hydrated with alcohol, eluted with PBS and placed in sodium citrate buffer (Solarbio) for antigen repair. The sections were blocked with goat serum (Solarbio) and incubated with primary antibodies of ki-67 (ab15580, 1:1000, Abcam) and ASCT2 (ab237704, 1:1600, Abcam) at room temperature for 1 h. Then, DBA color developer (Solarbio) and hematoxylin (Solarbio) were added to these sections for 2 min. After that, the slices were sealed by dehydration and observed under a microscope.

Statistical analysis

Data were analyzed using GraphPad Prism 7, and the results are presented as mean ± standard deviation. Differences between groups were analyzed using a student's *t*-test or analysis of variance (ANOVA). $p < 0.05$ was considered statistically significant.

RESULTS

CircCPA4 expression was upregulated in NSCLC tissues and cells

We noticed that circCPA4 expression was upregulated in NSCLC tissues and cells (A549 and H1299) compared to normal tissues and 16HBE cells (Figure 1a,b). Additionally, circCPA4 expression was significantly associated with tumor size, tumor node metastasis (TNM) stage and lymph node metastasis of NSCLC patients (Table S1). Figure 1c shows that circCPA4 is formed by the back-splicing of exons 7 and 10 of the CPA4 gene and is located on chromosome 7. Additionally, no obvious change in circCPA4 level was observed in A549 and H1299 cells treated with RNase R and actinomycin D, while the linear CPA4 was substantially degraded (Figure 1d,e). Altogether, these data suggest that a high level of circCPA4 may be associated with NSCLC progression.

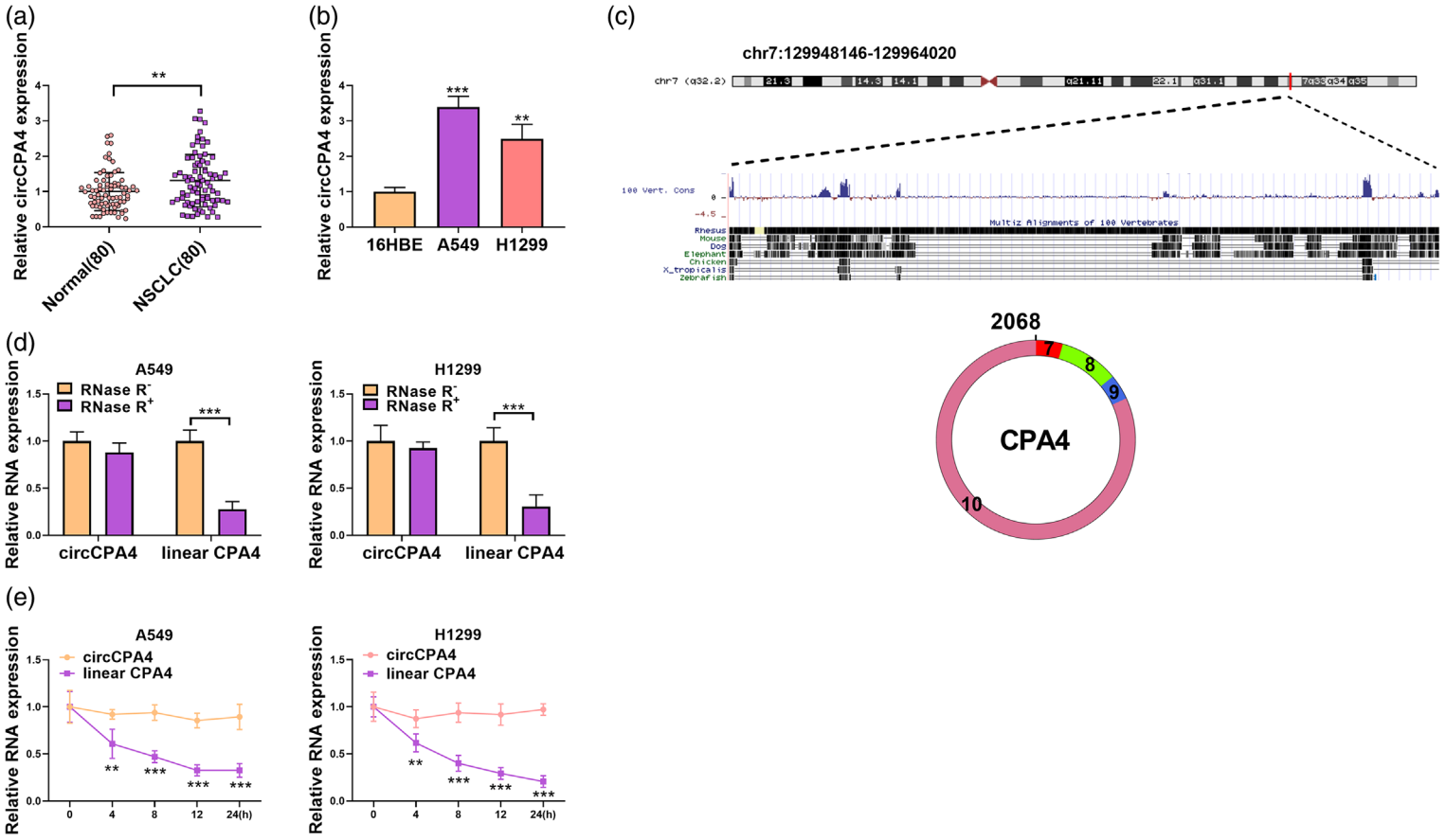

FIGURE 1 Expression characteristics of circCPA4 in non-small cell lung cancer (NSCLC). (a) The expression of circCPA4 in NSCLC tissues was measured by real-time quantitative polymerase chain reaction (RT-qPCR). (b) CircCPA4 abundance in A549 and H1299 cells was analyzed by RT-qPCR. (c) Schematic diagram of circCPA4 structure is shown. (d, e) RT-qPCR was utilized to analyze the levels of circCPA4 and linear CPA4 in A549 and H1299 cells after RNase R or actinomycin D treatment. $^{**}p < 0.01$ and $^{***}p < 0.001$.

CircCPA4 knockdown suppressed NSCLC cell proliferation, migration and invasion, but promoted apoptosis in vitro

A striking downregulation of circCPA4 was observed in NSCLC cells transfected with si-circCPA4 (Figure 2a). Then, si-circCPA4 was transfected into A549 and H1299 cells to examine the effect of circCPA4 knockdown on the malignant phenotypes of NSCLC cells. The CCK8 assay showed that the cell viability of the si-circCPA4 group was lower than that of the si-NC group (Figure 2b). Also, the EDU assay revealed that circCPA4 knockdown inhibited cell proliferation (Figure 2c). A549 and H1299 cells were transfected with si-circCPA4, and the apoptosis rate was greatly enhanced (Figure 2d). The transwell assay revealed that migration and invasion of A549 and H1299 cells were suppressed by circCPA4 silencing (Figure 2e,f). Wound-healing assay also showed that circCPA4 knockdown retarded the migration of A549 and H1299 cells (Figure 2g,h). Moreover, E-cadherin level was increased and vimentin level was decreased in A549 and H1299 cells after circCPA4 knockdown (Figure 2i). Overall, NSCLC cell function is restrained after circCPA4 knockdown.

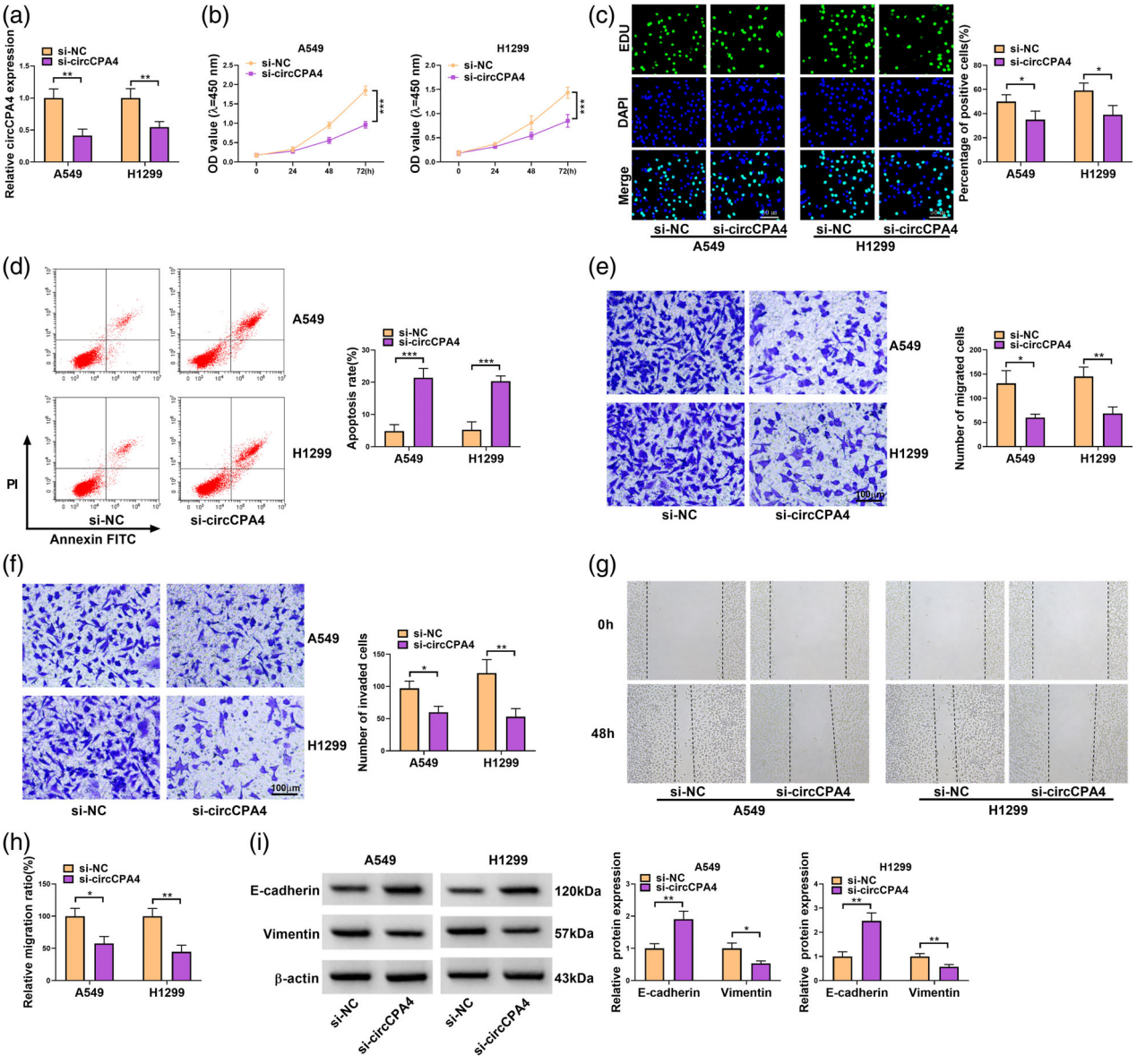

FIGURE 2 Silencing of circCPA4 inhibited the development of non-small cell lung cancer in vitro. (a) Real-time quantitative polymerase chain reaction was carried out to assess the effect of si-circCPA4 on circCPA4 expression. (b) Cell counting kit-8 assay was used to estimate cell viability of A549 and H1299 cells transfected with si-NC or si-circCPA4. (c) 5-ethynyl-2′-deoxyuridine assay was applied to analyze the proliferative capacity of A549 and H1299 cells transfected with si-NC or si-circCPA4. (d) Apoptosis rate of A549 and H1299 cells transfected with si-NC or si-circCPA4 was measured by a flow cytometer. (e, f) Transwell assay was conducted to detect migration and invasion of A549 and H1299 cells transfected with si-NC or si-circCPA4. (g, h) Wound-healing assay was performed to analyze migration of A549 and H1299 cells transfected with si-NC or si-circCPA4. (i) E-cadherin and vimentin protein levels were analyzed by western blot in A549 and H1299 cells transfected with si-NC or si-circCPA4. $^{*}p < 0.05$, $^{**}p < 0.01$ and $^{***}p < 0.001$.

CircCPA4 bound to miR-145-5p in NSCLC

The StarBase database showed that circCPA4 was able to bind to miR-145-5p, and their binding sites are illustrated in Figure 3a. In addition, we found a significant downregulation of luciferase activity in 293T cells cotransfected with circCPA4 wt and miR-145-5p mimic compared to the cotransfected group with circCPA4 wt and mimic NC (Figure 3b). Meanwhile, the phenomenon that circCPA4 and miR-145-5p had higher expression in the anti-Ago2 group compared to the anti-IgG group also supported the association between circCPA4 and miR-145-5p (Figure 3c). Next, we measured miR-145-5p level in 80 pairs of NSCLC tissue samples, and the results showed that miR-145-5p was at a lower level in NSCLC tissues (Figure 3d). MiR-145-5p and circCPA4 levels showed a negative correlation in NSCLC tissues (Figure 3e). MiR-145-5p expression was lower in NSCLC cells (A549 and H1299) than in 16HBE cells (Figure 3f). Overall, circCPA4 targets miR-145-5p in NSCLC cells.

CircCPA4 targeted miR-145-5p to modulate NSCLC progression

Rescue experiments were performed to test whether circCPA4 targeted miR-145-5p to regulate NSCLC cell progression. RT-qPCR results showed that transfection with miR-145-5p inhibitor effectively reduced miR-145-5p level in A549 and H1299 cells (Figure 4a). Moreover, the transfection with miR-145-5p inhibitor abrogated si-circCPA4-induced upregulation of miR-145-5p level in A549 and H1299 cells (Figure 4a,b). We observed that the inhibitory effect of si-circCPA4 on A549 and H1299 cell proliferation and its promoting effect on cell apoptosis were attenuated after the introduction of miR-145-5p inhibitor (Figure 4c–e). Meanwhile, circCPA4 silencing-induced inhibitory effects on migration and invasion of A549 and H1299 cells were reversed after miR-145-5p downregulation (Figure 4f–h). Finally, we also observed that miR-145-5p knockdown reversed the promoting effect on E-cadherin protein level and inhibitory effect on Vimentin protein level induced by circCPA4 downregulation (Figure 4i). Thus, these findings suggest that circCPA4 knockdown restrains the progression of NSCLC cells by targeting miR-145-5p.

ASCT2 was targeted by miR-145-5p in NSCLC

The binding sequences between ASCT2 and miR-145-5p were predicted by the StarBase database (Figure 5a). Next, luciferase reporter vectors including ASCT2 3′UTR wt and ASCT2 3′UTR mut were constructed and transfected into NSCLC cells with miR-145-5p mimic or mimic NC. The results of the dual-luciferase reporter assay showed that miR-145-5p inhibited the luciferase activity of the ASCT2 3′UTR wt group, whereas it had no notable effect on the luciferase activity of the ASCT2 3′UTR mut group (Figure 5b). ASCT2 mRNA level was significantly increased in NSCLC tissues in relative to normal tissues (Figure 5c). ASCT2 expression was negatively correlated with circCPA4 expression and positively with miR-145-5p

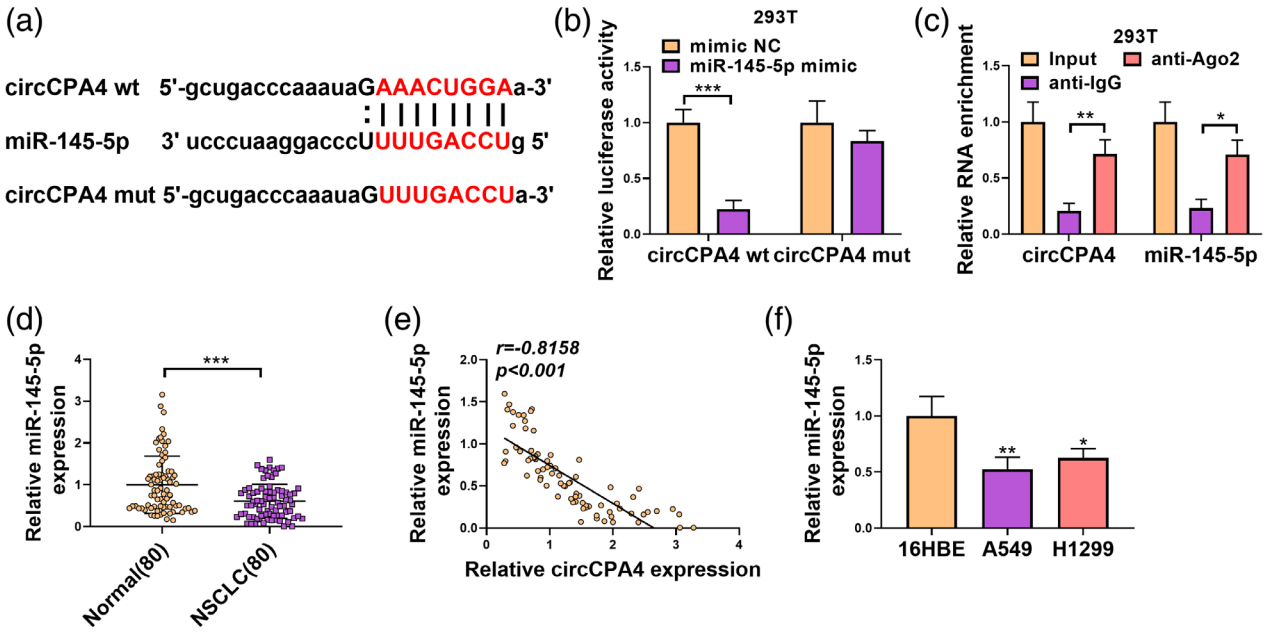

FIGURE 3 The association between circCPA4 and miR-145-5p was confirmed. (a) The binding sequences of circCPA4 for miR-145-5p are shown. (b) The association between circCPA4 and miR-145-5p was confirmed by a dual-luciferase reporter assay. (c) RNA immunoprecipitation assay was used to analyze the association between circCPA4 and miR-145-5p. (d) Real-time quantitative polymerase chain reaction (RT-qPCR) was executed to evaluate the level of miR-145-5p in 80 pairs of tissue samples. (e) Correlation between miR-145-5p and circCPA4 expression was determined by Pearson's correlation analysis in 80 pairs of non-small cell lung cancer (NSCLC) tissue samples. (f) The content of miR-145-5p in NSCLC and normal cells was analyzed by RT-qPCR. $^{*}p < 0.05$, $^{**}p < 0.01$ and $^{***}p < 0.001$.

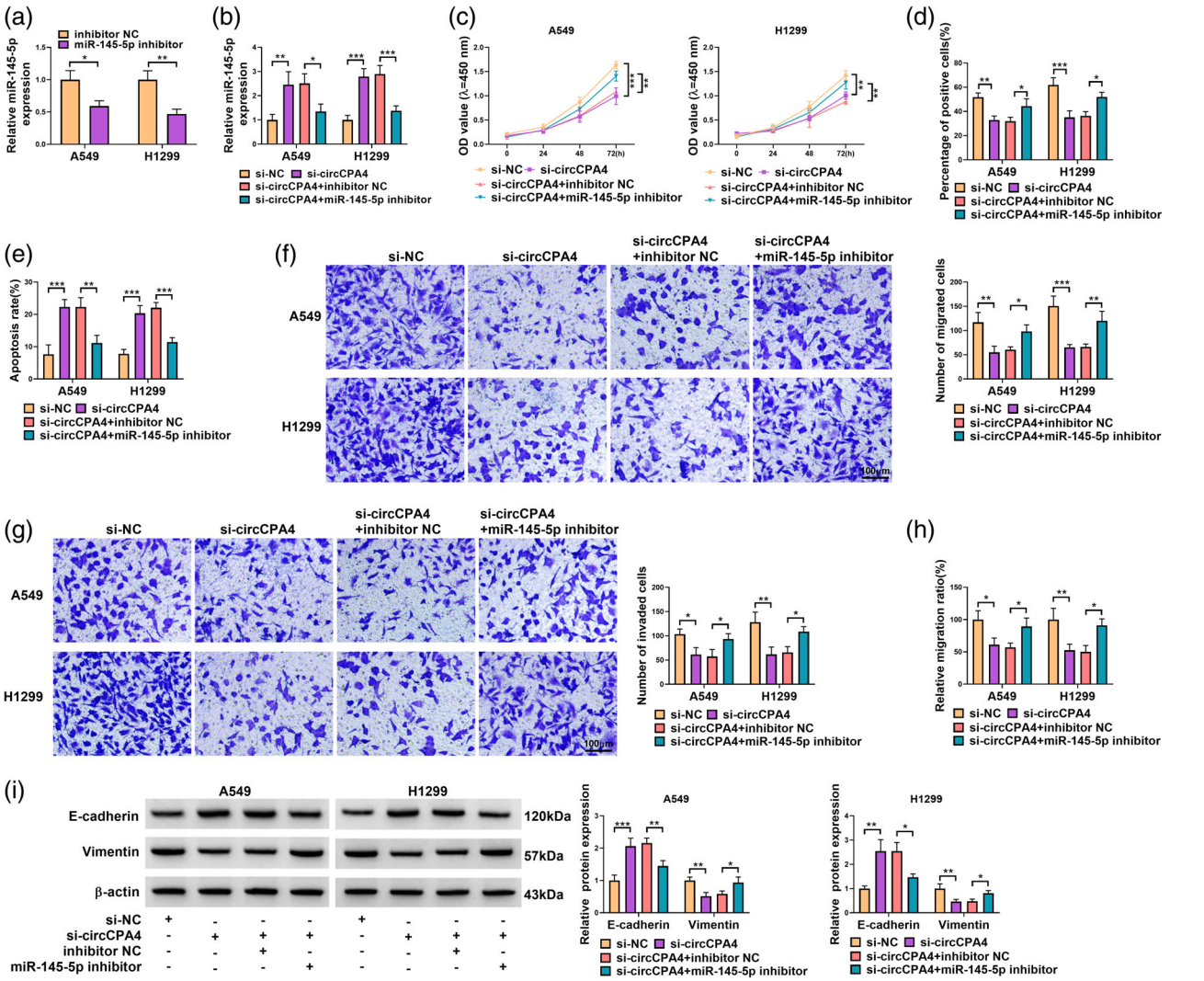

FIGURE 4 CircCPA4 regulated non-small cell lung cancer (NSCLC) cell function by adsorbing miR-145-5p. (a) The effect of miR-145-5p inhibitor on miR-145-5p expression was analyzed using real-time quantitative polymerase chain reaction (RT-qPCR). (b–i) Si-NC, si-circCPA4, si-circCPA4 + inhibitor NC, or si-circCPA4 + miR-145-5p inhibitor was transfected into A549 and H1299 cells. (b) RT-qPCR was used to analyze the level of miR-145-5p. (c, d) Cell counting kit-8 (CCK8) and 5′-ethynyl-2′-deoxyuridine (EdU) assays were performed to assess cell proliferation. (e) Apoptosis was detected by flow cytometry assay. (f, g) Transwell assay was conducted to detect A549 and H1299 cell migration and invasion. (h) Cell migration was examined using a wound-healing assay. (i) E-cadherin and vimentin protein levels were analyzed using western blot. $^{*}p < 0.05$, $^{**}p < 0.01$ and $^{***}p < 0.001$.

expression (Figure 5d,e). Also, ASCT2 protein level was markedly increased in NSCLC tissues and cells (A549 and H1299) (Figure 5f,g). Finally, the inhibitory effect of circCPA4 knockdown on ASCT2 protein level was restored by miR-145-5p inhibitor in A549 and H1299 cells (Figure 5h). These data suggest that ASCT2 is a downstream target of miR-145-5p and its expression is regulated by miR-145-5p and circCPA4.

ASCT2 upregulation diminished the effects of miR-145-5p overexpression on NSCLC cell progression

The efficiency of miR-145-5p mimic and pcDNA-ASCT2 in increasing miR-145-5p or ASCT2 expression in A549 and H1299 cells was confirmed in Figure 6a,b. Meanwhile, western blot data confirmed that the introduction of pcDNA-ASCT2 into A549 and H1299 cells reinstated the inhibitory effect of miR-145-5p overexpression on ASCT2 level (Figure 6c). Upregulation of miR-145-5p inhibited the proliferation of A549 and H1299 cells and accelerated apoptosis, however, ASCT2 overexpression abolished these effects (Figure 6d–f). In addition, we observed that miR-145-5p upregulation-induced inhibitory effects on migration and invasion were abolished by ASCT2 overexpression (Figure 6g–i). ASCT2 upregulation weakened the effect of miR-145-5p overexpression on E-cadherin and vimentin protein levels (Figure 6j). Further, the results showed that ASCT2 silencing inhibited A549 and H1299 cell proliferation, migration, and invasion and induced cell apoptosis (Figure S1a–f). Collectively, miR-145-5p modulated NSCLC cell progression by targeting ASCT2 in vitro.

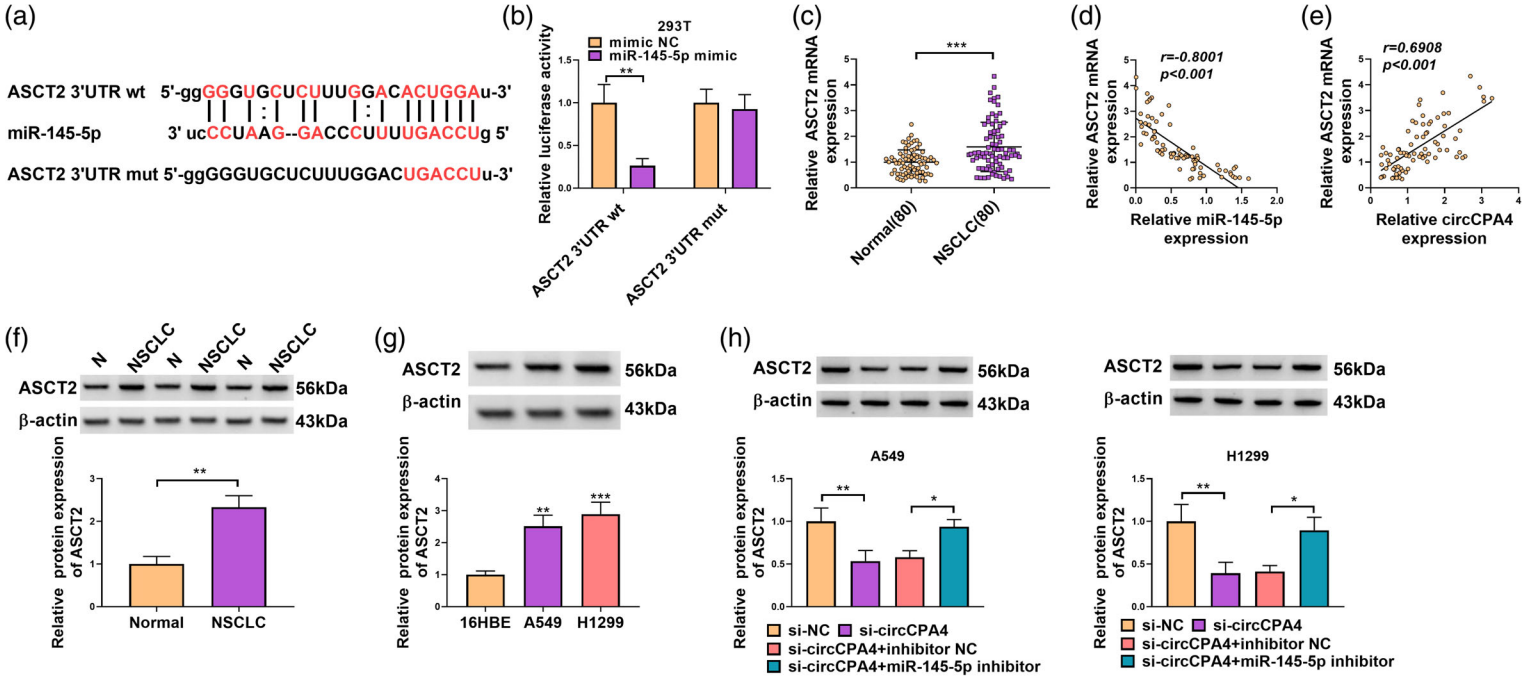

FIGURE 5 The association between ASCT2 and miR-145-5p was analyzed. (a) The binding sequences of ASCT2 for miR-145-5p are shown. (b) The correlation between ASCT2 and miR-145-5p was confirmed by a dual-luciferase reporter assay. (c) ASCT2 level in non-small cell lung cancer (NSCLC) tissues was measured by real-time quantitative polymerase chain reaction (RT-qPCR). (d, e) Pearson's correlation analysis was used to determine the correlation of ASCT2 with miR-145-5p and circCPA4 levels in NSCLC tissues. (f, g) The content of ASCT2 in NSCLC tissues and cells was detected by western blot assay. (h) A549 and H1299 cells were transfected with si-NC, si-circCPA4, si-circCPA4 + inhibitor NC, or si-circCPA4 + miR-145-5p inhibitor, and ASCT2 level was detected by RT-qPCR. $^{*}p < 0.05$, $^{**}p < 0.01$ and $^{***}p < 0.001$.

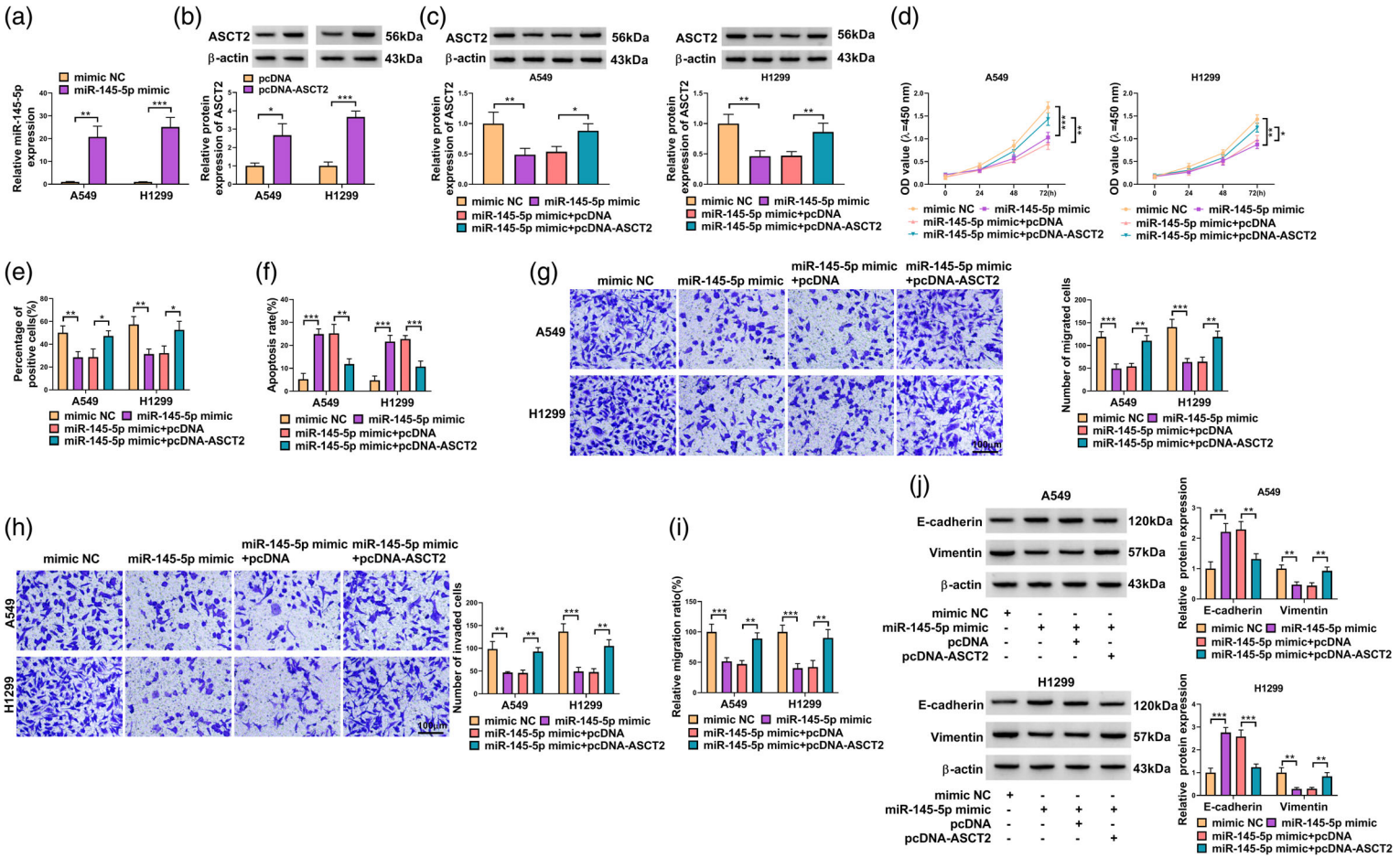

FIGURE 6 MiR-145-5p targeted ASCT2 to restrain non-small cell lung cancer (NSCLC) cell progression. (a) The miR-145-5p level in A549 and H1299 cells transfected with miR-145-5p mimic was measured using real-time quantitative polymerase chain reaction. (b) Overexpression efficiency of ASCT2 was measured using western blot. (c–j) A549 and H1299 cells were transfected with mimic NC, miR-145-5p mimic, miR-145-5p mimic+pcDNA or miR-145-5p mimic+pcDNA-ASCT2. (c) ASCT2 protein level was analyzed by western blot assay. (d, e) Cell counting kit-8 (CCK8) and 5′-ethynyl-2′-deoxyuridine (EdU) assays were performed to analyze the proliferation of A549 and H1299 cells. (f) Flow cytometry assay was performed to analyze cell apoptosis. (g, h) Migratory and invasive abilities of NSCLC cells were detected by transwell assay. (i) The migratory capacity of NSCLC cells was assessed by wound-healing assay. (j) E-cadherin and vimentin protein levels were examined by western blot. *$p < 0.05$, **$p < 0.01$ and ***$p < 0.001$.

CircCPA4 was involved in the regulation of intracellular glutamine level through miR-145-5p/ASCT2 axis in NSCLC cells

We observed distinct decreases in intracellular glutamine, glutamate and α-KG levels after circCPA4 silencing in A549 and H1299 cells; however, these phenomena were regained by miR-145-5p downregulation (Figure 7a–c). Additionally, ASCT2 upregulation relieved the inhibitory effects of miR-145-5p mimic on glutamine, glutamate and α-KG levels in A549 and H1299 cells (Figure 7d–f). These data indicated that circCPA4 downregulation decreased intracellular glutamine, glutamate and α-KG levels through the miR-145-5p/ASCT2 axis.

CircCPA4 knockdown repressed tumor growth in vivo

We evaluated the effect of circCPA4 silencing on tumor growth in vivo using a xenograft mouse model assay. After the injection of A549 cells stably transfected with sh-circCPA4 into mice, we observed that the tumor volume and weight of mice were substantially reduced in the sh-circCPA4 group when compared to the sh-NC group (Figure 8a,b). Furthermore, lower contents of circCPA4 and ASCT2 and high miR-145-5p level were detected in the tumor tissues of the sh-circCPA4 group (Figure 8c). Also, ASCT2 protein level in the tumor tissues of the sh-circCPA4 group was lower than that in the sh-NC group (Figure 8d). The immunohistochemistry (IHC) results showed a significant decrease in the expression of ASCT2 and ki-67 in tumor tissues from the sh-circCPA4 group in comparison with the tumor tissues from the sh-NC group (Figure 8e). These findings confirm that knockdown of circCPA4 leads to the arrest of tumor growth in vivo.

DISCUSSION

As research into the functional roles of circRNAs in disease progression continues to expand, there is mounting evidence supporting their potential as diagnostic or prognostic biomarkers for various diseases, including cancers.[25] In the present study, we identified that circCPA4 might be a reliable therapeutic target for NSCLC. Herein, our results showed that circCPA4 expression was upregulated in NSCLC and that it promoted the malignant behavior of NSCLC cells by enhancing cell proliferation, migration, and invasion while inhibiting cell apoptosis. Further investigations suggested that the regulatory effects of circCPA4 in NSCLC were associated with the circCPA4/miR-145-5p/ASCT2 pathway, a novel mechanism that has not been previously reported.

An early study has indicated that circCPA4 contributes to the aggressive progression of glioma.[26] Additionally, our

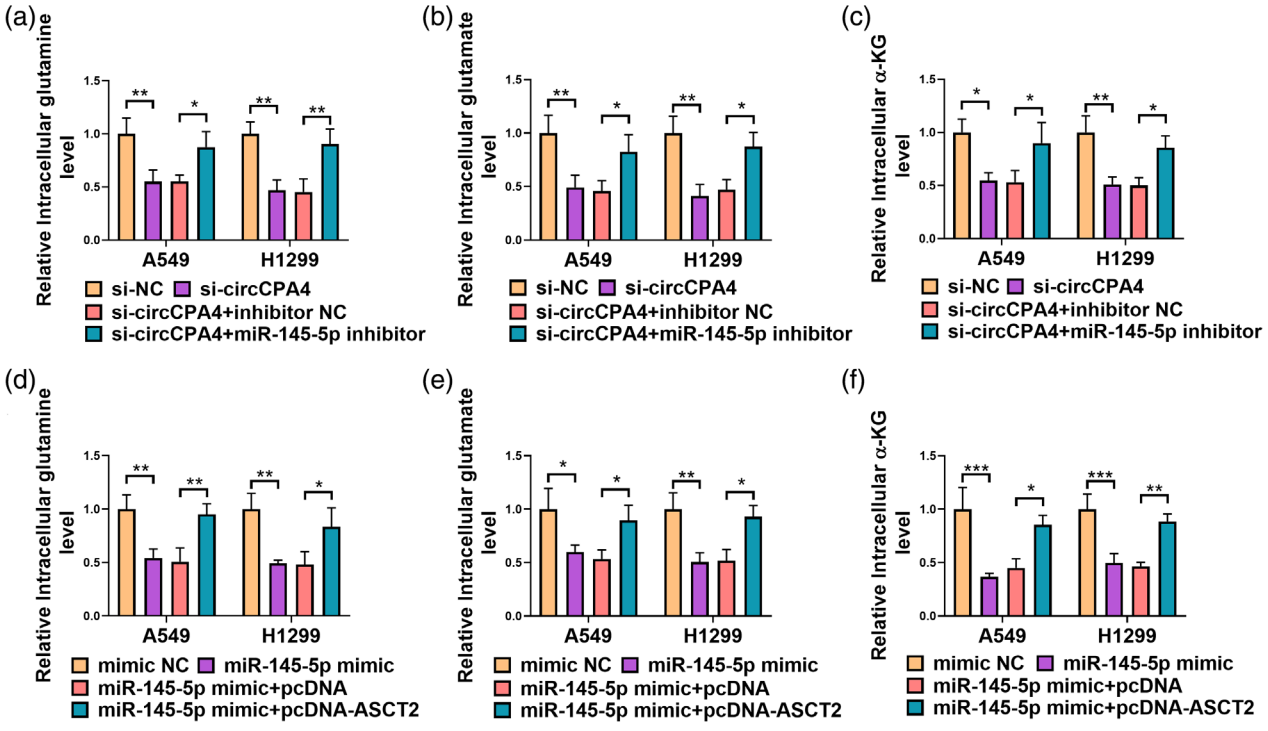

FIGURE 7 CircCPA4/miR-145-5p/ASCT2 axis regulated intracellular glutamine, glutamate and α-KG levels. (a–c) Si-NC, si-circCPA4, si-circCPA4 + inhibitor NC, and si-circCPA4 + miR-145-5p inhibitor were transfected into A549 and H1299 cells, and the corresponding kits were used to evaluate intracellular glutamine, glutamate and α-KG levels. (d–f) A549 and H1299 cells transfected with mimic NC, miR-145-5p mimic, miR-145-5p mimic+pcDNA and miR-145-5p mimic+pcDNA-ASCT2, and intracellular glutamine, glutamate and α-KG levels were detected by using the corresponding kits. $^{*}p < 0.05$, $^{**}p < 0.01$ and $^{***}p < 0.001$.

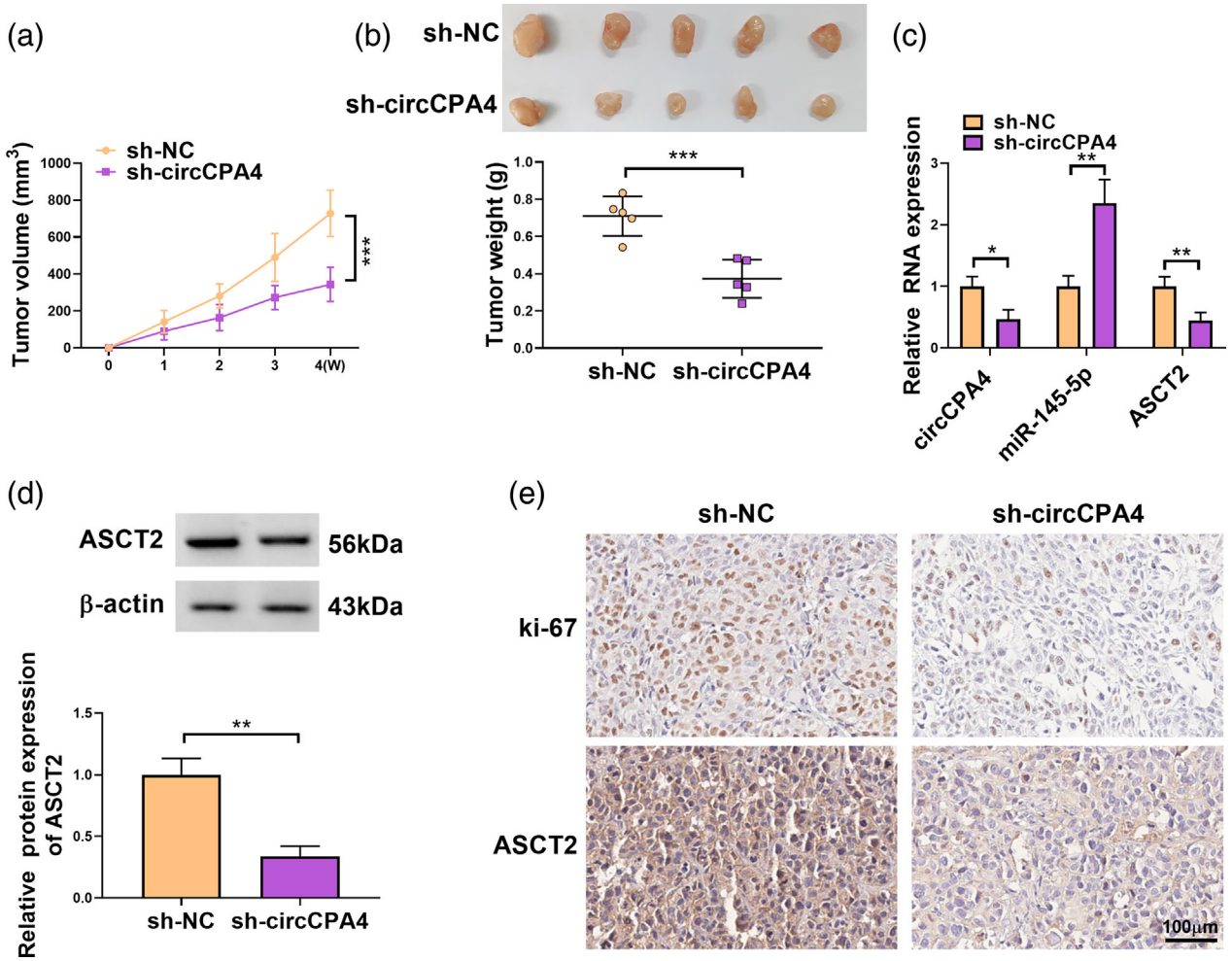

FIGURE 8 CircCPA4 silencing inhibited tumor growth in vivo. (a, b) Tumor volume and weight were measured in mice. (c, d) The contents of circCPA4, miR-145-5p and ASCT2 in tumor tissues were analyzed by real-time-quantitative polymerase chain reaction (RT-qPCR) and western blot assays. (e) ASCT2 and ki-67 levels in tumor tissues were measured using the IHC assay. $^{*}p < 0.05$, $^{**}p < 0.01$ and $^{***}p < 0.001$.

data aligned with the reports of high circCPA4 expression in NSCLC tissues and cells.[27] The current study provided evidence that knockdown of circCPA4 impeded the malignant progression of NSCLC cells in vitro, as well as in a mouse tumor model, corroborating existing literature on this topic.[13] The enhancement of glutamine metabolism is known to drive various cancer cell processes, and targeting glutamine metabolism has emerged as a potential therapeutic approach in cancer therapy.[28] In this study, we found that circCPA4 knockdown repressed intracellular glutamine, glutamate and α-KG levels in NSCLC cells. These findings, which have not been previously reported, highlight the involvement of circCPA4 in the regulation of glutamine metabolism in NSCLC.

The emerging concept of ceRNA suggests that circRNAs can competitively bind to miRNAs to mitigate their translational repression on target gene expression, thereby regulating cellular processes.[29] In line with this hypothesis, our results showed that circCPA4 bound to miR-145-5p to regulate NSCLC progression. Previous research has highlighted the dysregulation of miR-145-5p in various tumors, with evidence that it inhibits cancer development.[30–32] In our study, miR-145-5p expression was downregulated in NSCLC tissues, supporting earlier findings.[33] MiR-145-5p overexpression repressed cancer cell proliferation and metastasis, aligning with previous reports.[34,35] We also observed that miR-145-5p introduction inhibited intracellular glutamine, glutamate and α-KG levels and induced NSCLC cell apoptosis. Taken together, miR-145-5p emerges as a promising biomarker for disease diagnosis and prognosis, and its clinical utility for these purposes should be further explored.

MiR-145-5p was found to target ASCT2 in our study, and our study demonstrated that circCPA4 facilitated ASCT2 expression through miR-145-5p. The choice of ASCT2 as the target gene for miR-145-5p was made based on previous studies and evidence suggesting its potential involvement in the regulatory network of miR-145-5p. As reported, ASCT2 was dysregulated in cancers such as oral squamous cell carcinoma and endometrial carcinoma.[36,37] Meanwhile, the combination of ASCT2 inhibitor and other drugs may be a promising method in the future for cancer therapy.[38] ASCT2 is an essential transporter molecule in

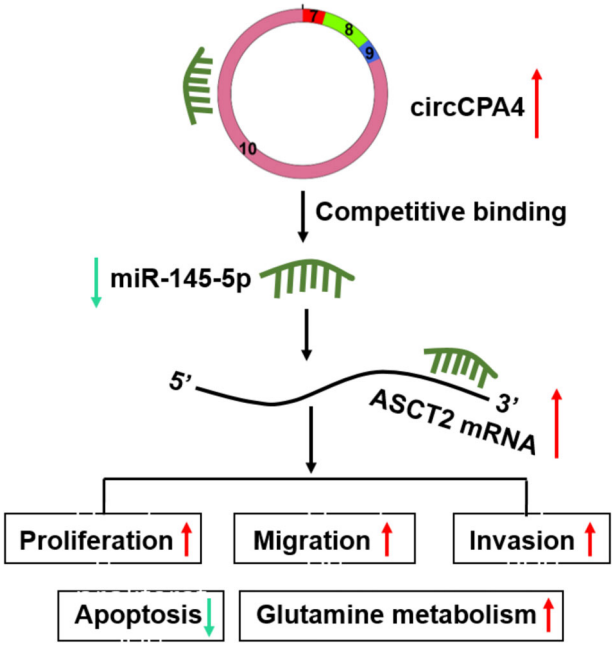

FIGURE 9 The schematic illustration showed the mechanism of circCPA4 regulating non-small cell lung cancer (NSCLC) cell malignancy. The increased expression of circCPA4 induced ASCT2 production through miR-145-5p, thereby promoting NSCLC cell proliferation, migration and invasion.

glutamine metabolism, and elevated ASCT2 expression was associated with enhanced glutamine metabolism.[39] In this study, we detected a significant upregulation of ASCT2 levels in 80 NSCLC tissues. ASCT2 overexpression reversed the inhibitory effects on intracellular glutamine, glutamate and α-KG levels and NSCLC cell malignant behaviors caused by miR-145-5p upregulation. Considerable evidence suggests that ASCT2 is a primary transporter for glutamine uptake and sustains the cytoplasmic amino acid pool to drive the function of LAT1, which enables transport of the essential amino acids to improve cancer cell growth through mTOR-induced translations.[40] Thus, circCPA4 regulated NSCLC cell malignancy through the miR-145-5p/ASCT2 pathway.

Our study analyzed the expression characteristics and regulatory role of ASCT2 in NSCLC, and our findings indicate that circCPA4 adsorbed miR-145-5p to upregulate ASCT2, thereby promoting NSCLC cell proliferation, metastasis and glutamine metabolism and inhibiting apoptosis (Figure 9). The result suggests that inhibition of circCPA4 expression may be a potential strategy for NSCLC therapy. However, the mouse model may not fully replicate the complex pathophysiology of human lung cancer, resulting in potential discrepancies in the response to circCPA4 treatment. Thus, alternative experimental approaches should be used to complement the drawbacks, such as patient-derived xenograft models. Additionally, the findings should be validated using external validation methods, and more experiments should be performed to delve deeper into the functional mechanism of circCPA4.

AUTHOR CONTRIBUTIONS

Conceptualization and methodology: Weiliang Liu and Tao Huang. Formal analysis and data curation: Junyan Li and Hui Hu. Validation and investigation: Xinyu Xu and Zhigang Fan. Writing–original draft preparation and writing–review and editing: Zhenhua Zhang, Weiliang Liu and Tao Huang. Approval of final manuscript: all authors.

FUNDING INFORMATION

This work was funded by Key R&D Plan of Shaanxi Province (2021SF-044).

CONFLICT OF INTEREST STATEMENT

The authors declare that they have no competing interests.

DATA AVAILABILITY STATEMENT

The datasets generated during and/or analyzed during the current study are available from the corresponding author on reasonable request.

ORCID

Zhigang Fan https://orcid.org/0009-0007-8856-2647

REFERENCES

1. Sung H, Ferlay J, Siegel RL, Laversanne M, Soerjomataram I, Jemal A, et al. Global cancer statistics 2020: GLOBOCAN estimates of incidence and mortality worldwide for 36 cancers in 185 countries. CA Cancer J Clin. 2021;71(3):209–49.
2. Le X, Nilsson M, Goldman J, et al. Dual EGFR-VEGF pathway inhibition: a promising strategy for patients with EGFR-mutant NSCLC. J Thorac Oncol. 2021;16(2):205–15.
3. Oudkerk M, Liu S, Heuvelmans MA, Walter JE, Field JK. Lung cancer LDCT screening and mortality reduction–evidence, pitfalls and future perspectives. Nat Rev Clin Oncol. 2021;18(3):135–51.
4. Mao Y, Yang D, He J, Krasna MJ. Epidemiology of lung cancer. Surg Oncol Clin N Am. 2016;25(3):439–45.
5. Chen LL. The biogenesis and emerging roles of circular RNAs. Nat Rev Mol Cell Biol. 2016;17(4):205–11.
6. Akhbari MH, Zafari Z, Sheykhhasan M. Competing endogenous RNAs (ceRNAs) in colorectal cancer: a review. Expert Rev Mol Med. 2022;24:e27.
7. Wu S, Lu J, Zhu H, Wu F, Mo Y, Xie L, et al. A novel axis of circKIF4A-miR-637-STAT3 promotes brain metastasis in triple-negative breast cancer. Cancer Lett. 2024;581:216508.
8. Xia F, Xie M, He J, Cheng D. Circ_0004140 promotes lung adenocarcinoma progression by upregulating NOVA2 via sponging miR-330-5p. Thorac Cancer. 2023;14(35):3483–94.
9. Arnaiz E, Sole C, Manterola L, Iparraguirre L, Otaegui D, Lawrie CH. CircRNAs and cancer: biomarkers and master regulators. Semin Cancer Biol. 2019;58:90–9.
10. Xu X, Zhang J, Tian Y, Gao Y, Dong X, Chen W, et al. CircRNA inhibits DNA damage repair by interacting with host gene. Mol Cancer. 2020;19(1):128.
11. Bi J, Liu H, Dong W, Xie W, He Q, Cai Z, et al. Circular RNA circ-ZKSCAN1 inhibits bladder cancer progression through miR-1178-3p/p21 axis and acts as a prognostic factor of recurrence. Mol Cancer. 2019;18(1):133.
12. Li J, Li Z, Jiang P, Peng M, Zhang X, Chen K, et al. Circular RNA IARS (circ-IARS) secreted by pancreatic cancer cells and located within exosomes regulates endothelial monolayer permeability to promote tumor metastasis. J Exp Clin Cancer Res. 2018;37(1):177.

13. Tao W, Cao C, Ren G, Zhou D. Circular RNA circCPA4 promotes tumorigenesis by regulating miR-214-3p/TGIF2 in lung cancer. Thorac Cancer. 2021;12:3356–69.
14. Vishnoi A, Rani S. MiRNA biogenesis and regulation of diseases: an overview. Methods Mol Biol. 2017;1509:1–10.
15. He Y, Wang Y, Liu L, Liu S, Liang L, Chen Y, et al. Circular RNA circ_0006282 contributes to the progression of gastric cancer by sponging miR-155 to upregulate the expression of FBXO22. Onco Targets Ther. 2020;13:1001–10.
16. Wu Q, Sun S, Li Z, Yang Q, Li B, Zhu S, et al. Tumour-originated exosomal miR-155 triggers cancer-associated cachexia to promote tumour progression. Mol Cancer. 2018;17(1):155.
17. Bi J, Liu H, Cai Z, Dong W, Jiang N, Yang M, et al. Circ-BPTF promotes bladder cancer progression and recurrence through the miR-31-5p/RAB27A axis. Aging (Albany NY). 2018;10(8): 1964–76.
18. Wei S, Zheng Y, Jiang Y, Li X, Geng J, Shen Y, et al. The circRNA circPTPRA suppresses epithelial-mesenchymal transitioning and metastasis of NSCLC cells by sponging miR-96-5p. EBioMedicine. 2019;44: 182–93.
19. Gan TQ, Xie ZC, Tang RX, Zhang TT, Li DY, Li ZY, et al. Clinical value of miR-145-5p in NSCLC and potential molecular mechanism exploration: a retrospective study based on GEO, qRT-PCR, and TCGA data. Tumour Biol. 2017;39(3):1010428317691683.
20. Masle-Farquhar E, Bröer A, Yabas M, Enders A, Bröer S. ASCT2 (SLC1A5)-deficient mice have normal B-cell development, proliferation, and antibody production. Front Immunol. 2017;8:549.
21. Cormerais Y, Massard PA, Vucetic M, Giuliano S, Tambutté E, Durivault J, et al. The glutamine transporter ASCT2 (SLC1A5) promotes tumor growth independently of the amino acid transporter LAT1 (SLC7A5). J Biol Chem. 2018;293(8):2877–87.
22. Liu Y, Zhao T, Li Z, Wang L, Yuan S, Sun L. The role of ASCT2 in cancer: a review. Eur J Pharmacol. 2018;837:81–7.
23. van Geldermalsen M, Wang Q, Nagarajah R, Marshall AD, Thoeng A, Gao D, et al. ASCT2/SLC1A5 controls glutamine uptake and tumour growth in triple-negative basal-like breast cancer. Oncogene. 2016; 35(24):3201–8.
24. Zheng H, Fu Q, Ma K, Shi S, Fu Y. Circ_0079558 promotes papillary thyroid cancer progression by binding to miR-26b-5p to activate MET/AKT signaling. Endocr J. 2021;68(11):1247–66.
25. Shang Q, Yang Z, Jia R, Ge S. The novel roles of circRNAs in human cancer. Mol Cancer. 2019;18(1):6.
26. Zhang Y, Cai Z, Liang J, Chai E, Lu A, Shang Y. CircCPA4 promotes the malignant phenotypes in glioma via miR-760/MEF2D Axis. Neurochem Res. 2020;45(12):2903–13.
27. Hong W, Xue M, Jiang J, Zhang Y, Gao X. Circular RNA circ-CPA4/let-7 miRNA/PD-L1 axis regulates cell growth, stemness, drug resistance and immune evasion in non-small cell lung cancer (NSCLC). J Exp Clin Cancer Res. 2020;39(1):149.
28. Cluntun AA, Lukey MJ, Cerione RA, Locasale JW. Glutamine metabolism in cancer: understanding the heterogeneity. Trends Cancer. 2017; 3(3):169–80.
29. Zhong Y, Du Y, Yang X, et al. Circular RNAs function as ceRNAs to regulate and control human cancer progression. Mol Cancer. 2018; 17(1):79.
30. Chen J, Chen T, Zhu Y, Li Y, Zhang Y, Wang Y, et al. circPTN sponges miR-145-5p/miR-330-5p to promote proliferation and stemness in glioma. J Exp Clin Cancer Res. 2019;38(1):398.
31. Liang H, Sun H, Yang J, Yi C. miR-145-5p reduces proliferation and migration of hepatocellular carcinoma by targeting KLF5. Mol Med Rep. 2018;17(6):8332–8.
32. He S, Yu G, Peng K, Liu S. MicroRNA-145-5p suppresses fascin to inhibit the invasion and migration of cervical carcinoma cells. Mol Med Rep. 2020;22(6):5282–92.
33. Zhu Z, Wu Q, Zhang M, Tong J, Zhong B, Yuan K. Hsa_circ_0016760 exacerbates the malignant development of non-small cell lung cancer by sponging miR-145-5p/FGF5. Oncol Rep. 2021;45(2):501–12.
34. Tuo Z, Liang L, Zhou R. LINC00852 is associated with poor prognosis in non-small cell lung cancer patients and its inhibition suppresses cancer cell proliferation and chemoresistance via the hsa-miR-145-5p/KLF4 axis. J Gene Med. 2021;23(12):e3384.
35. Yu C, Li B, Wang J, Zhang Z, Li S, Lei S, et al. miR-145-5p modulates gefitinib resistance by targeting NRAS and MEST in non-small cell lung cancer. Ann Clin Lab Sci. 2021;51(5):625–37.
36. Luo Y, Li W, Ling Z, Hu Q, Fan Z, Cheng B, et al. ASCT2 overexpression is associated with poor survival of OSCC patients and ASCT2 knockdown inhibited growth of glutamine-addicted OSCC cells. Cancer Med. 2020;9(10):3489–99.
37. Marshall AD, van Geldermalsen M, Otte NJ, Lum T, Vellozzi M, Thoeng A, et al. ASCT2 regulates glutamine uptake and cell growth in endometrial carcinoma. Oncogenesis. 2017;6(7):e367.
38. Teixeira E, Silva C, Martel F. The role of the glutamine transporter ASCT2 in antineoplastic therapy. Cancer Chemother Pharmacol. 2021;87(4):447–64.
39. Schulte ML, Fu A, Zhao P, Li J, Geng L, Smith ST, et al. Pharmacological blockade of ASCT2-dependent glutamine transport leads to antitumor efficacy in preclinical models. Nat Med. 2018;24(2):194–202.
40. Fuchs BC, Bode BP. Amino acid transporters ASCT2 and LAT1 in cancer: partners in crime? Semin Cancer Biol. 2005;15(4):254–66.

SUPPORTING INFORMATION

Additional supporting information can be found online in the Supporting Information section at the end of this article.

How to cite this article: Zhang Z, Liu W, Huang T, Li J, Hu H, Xu X, et al. CircCPA4 induces ASCT2 expression to promote tumor property of non-small cell lung cancer cells in a miR-145-5p-dependent manner. Thorac Cancer. 2024;15(10):764–77. https://doi.org/10.1111/1759-7714.15257